Observational limitations of Bose-Einstein photon statistics and radiation noise in thermal emission

Y.-J. Lee and J. J. Talghader

Phys. Rev. A **97**, 013844 — Published 26 January 2018

DOI: 10.1103/PhysRevA.97.013844

Observational Limitations of Bose-Einstein Photon Statistics and Radiation Noise in Thermal Emission

Y.-J. Lee[1], and J. J. Talghader[1]*
[1]*Department of Electrical and Computer Engineering, University of Minnesota, Minneapolis, MN 55455, USA*
(Received 7 August 2017; revised manuscript received 12 December 2017)

For many decades, theory has predicted that Bose-Einstein statistics are a fundamental feature of thermal emission into one or a few optical modes; however, the resulting Bose-Einstein-like photon noise has never been experimentally observed. There are at least two reasons for this: 1) relationships to describe the thermal radiation noise for an arbitrary mode structure have yet to be set forth, and 2) the mode and detector constraints necessary for the detection of such light is extremely hard to fulfill. Herein, photon statistics and radiation noise relationships are developed for systems with any number of modes and couplings to an observing space. The results are shown to reproduce existing special cases of thermal emission and are then applied to resonator systems to discuss physically realizable conditions under which Bose-Einstein-like thermal statistics might be observed. Examples include a single isolated cavity and an emitter cavity coupled to a small detector space. Low mode-number noise theory shows major deviations from solely Bose-Einstein or Poisson treatments and has particular significance because of recent advances in perfect absorption and subwavelength structures both in the long-wave infrared and terahertz regimes. These microresonator devices tend to utilize a small volume with few modes, a regime where the current theory of thermal emission fluctuations and background noise, which was developed decades ago for free space or single-mode cavities, has no derived solutions.

PACS numbers: 44.40.+a, 42.50.Ar, 05.30.Jp, 02.50.Cw

I. INTRODUCTION

Fundamental treatments of photon noise indicate that thermal emission noise follows Bose-Einstein (BE) statistics rather than Poisson. It is often pointed out that BE behavior is lost or reduced in systems where the thermal emission interacts with many modes, which is a feature of almost every practical implementation. However, even after decades of advances in thermal emitters and photon and thermal detectors, it is still not clear that BE-like noise for thermal light has ever been observed [1–4]. One difficulty with making such an observation is that a thermally emitting (or detecting) cavity almost never perfectly couples to just one single mode. Even the highest finesse cavities typically interact with a large number of free-space or external cavity modes, which introduce loss and/or averaging that creates a more Poisson-like statistical behavior. A second difficulty is that systems with few interacting modes are difficult to treat mathematically, and a general solution for thermal statistics in a cavity with an arbitrary mode structure and coupling has only been developed recently. In this paper, we develop relationships describing radiation noise for free space and internal to microcavities. We further analyze in detail the possibility of observing BE-like photon statistics in micro-cavities and resonators coupled to thermal emission or detection systems with any arbitrary mode structure and coupling.

*Present address: 4–174 Keller Hall, 200 Union St. SE, Minneapolis, MN 55455, USA; joey@umn.edu

The quantum thermal emission law developed by Planck is one of the pillars of modern physics; however, it must be modified when applied to micro- and nano-systems, where the emitting or absorbing object has a size comparable to or less than that of a wavelength [5,6]. For many devices on this scale, such as detectors, fluctuations are even more important than the base level of the emission, since fluctuations set the ultimate ability of the device to distinguish a signal from the thermal radiation background. The early work on fluctuations [7–13] was performed decades ago on objects and devices interacting with either idealized single modes or the many modes of free space. For the former, photon number fluctuations appear Poisson-like for wavelengths near to and shorter than the thermal emission maximum, while they follow BE-like statistics at very long wavelengths. As discussed above, the presence of many modes averages the BE contribution of each individual mode, resulting in Poisson-like fluctuations.

A fraction of the early work on energy fluctuations and background noise ignored the randomizing nature of many mode systems and contained errors [7,9,11] that have propagated into later treatments and textbooks down to the present day [14–16]. Later treatments of photon statistics and radiation noise [17–19] have handled thermal emission fluctuations for a few additional special cases, most notably that of a system with a number of uniform modes [11,12]. This work discussed the difficulty of a obtaining a general solution for a system with an arbitrary mode structure.

Olson, et. al. [20] developed a solution for photon number fluctuations for an idealized arbitrary cavity mode structure, but did not analyze the radiation background noise or the conditions under which BE-like statistics might be observed.

Despite the progress of these many authors, there remains no general treatment of thermal emission energy fluctuations and radiation noise for objects interacting with an arbitrary mode structure. In previous decades, this was an acceptable situation since nearly all existing devices interacted with many modes. However, there are currently many structures and devices that have *both* high spectral selectivity and volumes comparable to or smaller than λ^3, where λ is the wavelength of light. This combination of properties drives the number of cavity modes downward and makes the relative coupling of each mode to free space (or external cavity) modes of paramount importance. Recent devices with both narrow spectrum and small volume include microresonators [21,22], microcavity detectors [23,24], microcavity emitters and lasers [25,26], perfect absorbers [27,28], and others. Perhaps the most classic example is a narrow spectrum thermal emitter. This is shown conceptually in Fig. 1 coupled to a detector in (a) the same cavity, and (b) an external cavity, to measure the fluctuations. While the physical devices shown in Fig. 1 ostensibly apply to infrared systems, the physical treatment that we discuss applies equally well to terahertz (THz) systems, and the Fabry-Perot cavity in the diagram could be replaced with an appropriate THz resonator. Indeed, BE noise becomes most clearly dominant in the single-mode thermal THz regime. We now turn to an analysis the nature of the radiation background noise that would be observed for a general system.

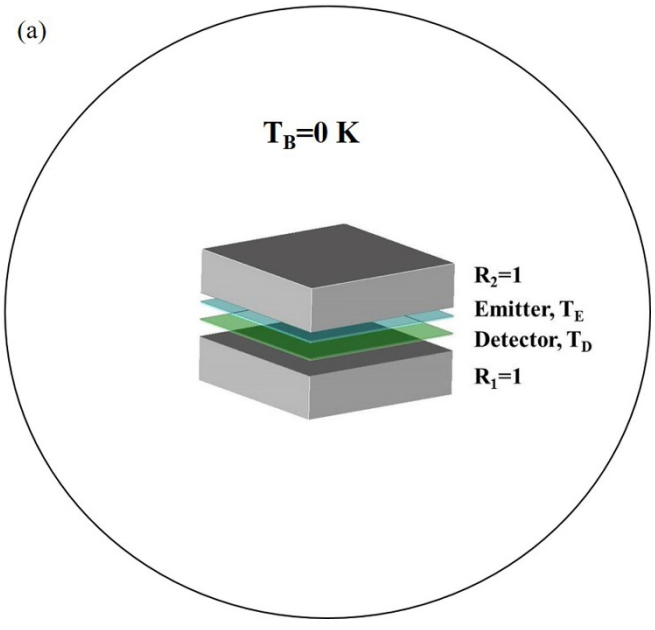

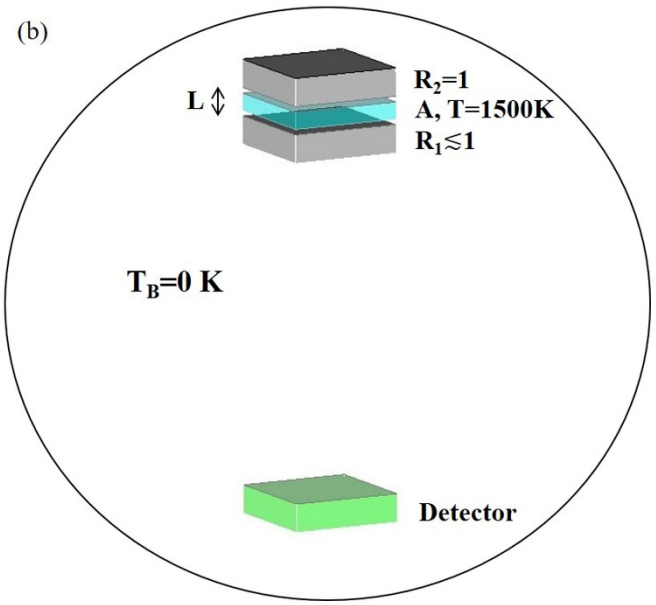

FIG. 1 (color online). Conceptual diagram of a resonator-based thermal emitter that couples to a detector in (a) the same cavity and (b) an external cavity.

II. DERIVATION AND ANALYSIS OF THERMAL EMISSION ENERGY FLUCTUATIONS WITH A SPECTRALLY DEPENDENT MODE STRUCTURE

Thermal emission energy fluctuations result from time dependent variations in the number of photons emitted from or absorbed by a physical object at a temperature above absolute zero. Over a small frequency range, the square of the thermal emission energy fluctuations of an object can be expressed by multiplying the density of states, square of the photon energy, photon number variance, and volume. For a blackbody in free space, the mode density is $\frac{8\pi\nu^2}{c^3}d\nu$ and the resulting equation is:

$$\left\langle \Delta E^2 \right\rangle = \iint \frac{2\nu^2}{c^3} \left(h\nu\right)^2 \left\langle \Delta n^2 \right\rangle V d\nu d\Omega \qquad (1)$$

where $\left\langle \Delta E^2 \right\rangle$ represents the mean squared energy fluctuation (variance), ν is the photon frequency, c is the speed of light, h is Planck's constant, Ω is solid angle, and $\left\langle \Delta n^2 \right\rangle$ represents the total photon number variance. At this point, the only restriction on the volume, V, is that it is very large with respect to wavelength. Also note that $\left\langle \Delta n^2 \right\rangle$ can be (and is) temperature and frequency dependent.

At very small volumes, where V ~ λ^3 , the distribution of cavity modes deviates substantially from that of free space. The exact mathematical treatment of the mode structure of a microcavity will be highly geometry dependent, but in principle one merely counts the number of modes of the cavity in the spectral range of interest and sums the product of energy squared and photon number variance over each one:

$$\left\langle \Delta E^2 \right\rangle = \sum_{\mathrm{m}} \left(h\nu_m\right)^2 \left\langle \Delta n^2 \right\rangle_{\mathrm{m}} \tag{2}$$

Since energy fluctuations increase linearly with volume, plots of $\left\langle \Delta E^2 \right\rangle$ will usually be normalized by this factor for easier comparison across size scales.

For an object interacting with a single optical mode, the photon number fluctuations satisfy Bose-Einstein statistics [29], such that $\left\langle \Delta n^2 \right\rangle_{\mathrm{m}} = \left\langle n_m \right\rangle + \left\langle n_m \right\rangle^2$, where $\left\langle n_m \right\rangle$ is the average photon number in the single mode, m, in the volume of the system. At the opposite extreme is a system with many modes, where thermal emission photons populate the system so that the combined photon statistics become Poisson-like, i.e. $\left\langle \Delta n^2 \right\rangle = \left\langle n \right\rangle$, where $\left\langle \Delta n^2 \right\rangle$ and $\left\langle n \right\rangle$ are the photon number variance and average number, respectively, for all modes combined. Between these extremes is the general case of an arbitrary number of modes, most commonly seen in micro- and nano-cavities.

Note that the variance represents the second statistical moment. Two distribution functions could have identical variances but differ in higher-order moments, such as skewness or kurtosis [29]. Therefore, we will use the terms, "Poisson-like" and "BE-like" in this paper to discuss systems with a variance near $\left\langle n \right\rangle$ or $\left\langle n \right\rangle + \left\langle n \right\rangle^2$ respectively.

To see how this develops, we note that the average total number of photons must be equal to the sum of the averages for all of the modes, $\left\langle n \right\rangle = \sum_m \left\langle n_m \right\rangle$. This is true for any general emitter/absorber (not necessarily a blackbody). For thermal emission of a blackbody in equilibrium, we can use the standard equation for the average number of photons in a mode found in many thermodynamics texts [30,31]:

$$\left\langle n_m \right\rangle_{BB} = \frac{1}{e^{\frac{h\nu}{kT}} - 1} \tag{3}$$

If a thermal emitter (or, equivalently, absorber) is not a blackbody, then this equation will be modified by the emissivity, i.e. the coupling strength of the graybody to a specific mode. The expression then becomes:

$$\left\langle n_m \right\rangle = \frac{\varepsilon_{\mathrm{m}}}{e^{\frac{h\nu}{kT}} - 1} \tag{4}$$

or equivalently, $\left\langle n_m \right\rangle = \varepsilon_{\mathrm{m}} \left\langle n_m \right\rangle_{BB}$. If we use these expressions of photon number in a Bose-Einstein probability distribution, the photon number variance for a system with an arbitrary mode structure takes the form [20],

$$\left\langle \Delta n^2 \right\rangle = \left\langle n \right\rangle + \frac{\left\langle n \right\rangle^2}{M_{eff}} = \sum_m \left(\left\langle n_m \right\rangle + \left\langle n_m \right\rangle^2 \right) \tag{5}$$

where

$$\frac{1}{M_{eff}} = \frac{\sum_m \left\langle n_m \right\rangle^2}{\left(\sum_m \left\langle n_m \right\rangle \right)^2} \tag{6}$$

Here M_{eff} is the effective number of modes. As one would expect, M_{eff} is a parameter that describes the number of modes interacting with a thermal system, but it differs from the simple mode number because it incorporates different strengths of coupling between the thermal emitter/absorber and each mode. For example, consider the discrete distribution of modes in Fig. 2. In Fig. 2, the interaction strength of each mode differs from the others. This means that the population of thermally emitted photons into of these modes will be less than predicted from Planck's Law for that frequency and temperature. However, if it has a uniform set of modes, each mode has identical strength (for example, each mode with strength equal to blue dash line) and M_{eff} is obtained merely by counting each one.

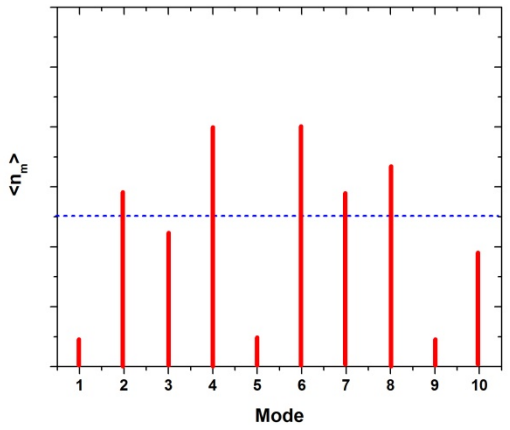

FIG. 2 (color online). Conceptual diagram of a system of modes with different couplings to a thermal emitter for each mode. The effective mode number, M_{eff}, must be calculated using an average photon number that is weighted by the coupling, or emissivity, of each mode (see Eqns (4) and (6)), or else theory will underestimate the magnitude of BE noise. Blue dash line shows a uniform coupling for each mode with identical strength.

We can draw several critical conclusions about thermal emission from this analysis:

1) As stated previously, a single mode system will have Bose-Einstein photon statistics while a many mode system in aggregate will have Poisson-like photon number fluctuations. However, *each individual mode of a multiple mode system will have Bose-Einstein statistics, regardless of the system statistics in aggregate.*
2) Any random sample of the photons of a system with Bose Einstein statistics will also have Bose-Einstein statistics. For example, consider a single mode microresonator that randomly scatters a small fraction of the photons propagating within it out into free space. These scattered photons in aggregate will also have BE statistics (but as will be discussed, a low number density may make the distinction between Poisson-like and BE-like photon number fluctuations difficult to see).
3) Emissivity must be considered per mode prior to the calculation of $\langle \Delta n^2 \rangle$. Often in the literature, one sees photon number fluctuations calculated using a modified Eqn (5), where $\langle \Delta n^2 \rangle$ for a blackbody is directly multiplied by $\varepsilon(\nu,\Omega)$, but this calculation is not correct. Granted, it has negligible errors at wavelengths equal to or shorter than the peak thermal emission wavelength, but it can have significant errors for individual (or few) modes at wavelengths significantly longer than the thermal emission peak. The proper expression is:

$$\langle \Delta n^2 \rangle = \sum_{\mathrm{m}} \langle n_m \rangle + \langle n_m \rangle^2 = \sum_{\mathrm{m}} \left[\frac{\varepsilon_m}{e^{\frac{h\nu}{kT}} - 1} + \left(\frac{\varepsilon_m}{e^{\frac{h\nu}{kT}} - 1} \right)^2 \right] \quad (7)$$

4) The frequency spacing between modes does not affect the photon number fluctuations except through the emissivity (i.e. coupling) of each mode and the natural frequency dependence of Planck's Law. In other words, two modes separated by 1nm in wavelength would have the same number fluctuations as two separated by 2nm unless the emissivity or population significantly changed over that wavelength range.
5) The BE-like statistics of a single mode of a many mode system may be difficult to distinguish from Poisson-like statistics. First, the spectral resolution necessary to see a single mode is extremely high. Second, since $\langle n_m \rangle$ is only a small fraction of $\langle n \rangle$, the magnitude of the $\langle n_m \rangle^2$ term will be extremely small compared to $\langle n \rangle^2$. This is particularly true for common visible wavelength ranges, where the average population of photons in a mode as given by Eqn (4) is much less than 1 and distinguishing $\langle n_m \rangle + \langle n_m \rangle^2$ from $\langle n_m \rangle$ could be impractical. Conversely, a few mode system working at long wavelengths and elevated temperatures could allow BE-like statistics to be seen by sampling a fraction of the spectral range of the overall thermal system.
6) The numbers of modes are not determined solely by the isolated detector or emitter volumes (if they are separated into different cavities), but rather by the total mode structure of the coupled emitter-detector system. For example, a heated single mode cavity emitting toward a detector in free space would not be single mode for purposes of photon statistics and radiation noise since multiple free space modes will couple with the emitting cavity mode.
7) Quantum vacuum fluctuations will contribute a large part of the overall electric field at low temperatures since the number of thermal photons will be very small. This is seen in numerous cavity effects, such as the Jaynes-Cummings line splitting[31]. However, an analysis of the thermal photon statistics, by necessity, utilizes the fluctuations in detected photon number. Since the vacuum fluctuations are virtual, they cannot themselves contribute to the number of directly

detected photons. However, along with radiation reaction[32], these same vacuum fluctuations play a major role in stimulating thermal spontaneous emission transitions, which represent the $\langle n \rangle$ term in the photon number variance $\langle n \rangle + \langle n \rangle^2$. The $\langle n \rangle^2$ term represents stimulated thermal emission.

III. OBSERVING BOSE-EINSTEIN STATISTICS IN THERMAL EMISSION

From the previous discussion, it is clear that only thermal systems with a single mode or few modes will ever be observed to have BE-like. This condition is usually extremely difficult to produce in practice. Recall the simple case of a spectrally narrow heated device emitting into free space, where the radiation noise is measured by an ideal detector. The number of modes in a spectral region in free space is given by $\frac{8\pi v^2 V}{c^3} dv$. For a typical-size laboratory, where $V = (3m)^3$, and an emission wavelength and frequency of $\lambda = 5\mu m$ and 60THz, respectively, the spectral resolution of an emitting cavity would have to be narrower than about 2.3 x 10^{-5} Hz in order for the emitted photons to be confined to a single free space mode. This corresponds to a microcavity finesse on the order of or exceeding 10^{18}, which is many orders of magnitude beyond experimentally achievable values [33–35].

Therefore, in order to have few modes, not only must the emitter be confined to a small volume, but the detector interactions with its enclosing volume, whether large or small, must be considered as well. The emitter and detector can either be confined to the same cavity (volume), or they can be separated into two coupled volumes. We will consider each case in turn below.

A. Observing Bose Einstein radiation background noise within a single cavity

A single cavity containing an emitter and detector was shown in Fig. 1(a). The diagram is of an infrared Fabry-Perot cavity, but for generality, it could be replaced with a THz resonator also containing a detector and emitter. This cavity is ideal, one-dimensional, and lossless, having mirrors of 100% reflectivity, and the space in which it resides has perfectly absorbing walls and is held at absolute zero. This space can have any volume but to place a lower bound on the observability of BE-like noise, it will be considered infinitely large. Smaller volumes will confine the lateral dimensions and, because of the smaller mode density with create fewer interactions with non-cavity axis modes. With perfectly reflective mirrors, the finesse of the cavity is defined by the absorption of the emitter and detector. The detector and emitter have been placed between the two mirrors, for example, each at a different intensity peak in the standing wave patterns within the cavity for maximum coupling. Other positions within the cavity or as part of the mirrors are possible with appropriate adjustments of the coupling calculations. It is important to note that the cavity system may have many modes in total; however, the emitter and detector will interact most strongly through the cavity modes defined along the cavity axis because radiation emitted in other directions will be immediately absorbed by the walls of the already-mentioned enclosing space held at absolute zero.

Let the emitter have a single-pass absorption, A/2, and a temperature T_E and the detector have the same absorption but temperature, T_D. The finesse of this cavity can be calculated [36] to be $F = \frac{\pi\sqrt{1-A}}{A}$. (Note that equal absorptions are merely a simplification and not a necessary condition for the analysis below.) In order to best identify energy fluctuations of the emitter, the detector temperature must be low, assisted by cryogenically cooling the entire cavity system to near absolute zero. The emitter temperature must be raised to a high value by, say, joule or inductive heating. We note that in reality for a fully confined, lossless cavity, it would be impossible to raise the emitter temperature by external means because no connection to the outside world would be allowed; however, for purposes of this example we will assume that heating takes place, for example, inductively via a frequency far from the resonance or via joule heating with wires aligned away from the cavity axis, so that the system can be considered lossless along the cavity axis over the (narrow) spectral absorption range of the detector.

Some sort of external attachment to the detector is also necessary for both the logical reason that there must be some means to hold it in place and read out the signal and the fundamental reason that the detector must be cooled because in a system solely limited by radiation heat transfer, radiation coupling along the cavity axis will raise the temperature of the detector to levels that would make seeing the energy fluctuations of a single emitter mode impossible. Let us examine this latter point in more detail.

The temperatures T_E and T_D are not independent because they are coupled via thermal radiation emitted within the cavity resonance, and the detector must absorb light of this frequency and direction or else the

noise characteristics cannot be determined. If the cavity heat transfer is completely radiation-limited, the temperature of the detector can be written as a function of the background and emitter temperatures as:

$$\sum_{\mathrm{m}} \frac{\varepsilon_{ED} h\nu}{e^{\frac{h\nu}{kT_E}}-1} + \int_0^\infty \int_{\Omega_{space}} \frac{2\nu^2}{c^3} \frac{\varepsilon_D h\nu}{e^{\frac{h\nu}{kT_B}}-1} d\Omega d\nu$$
$$= \sum_{\mathrm{m}} \frac{\varepsilon_{ED} h\nu}{e^{\frac{h\nu}{kT_D}}-1} + \int_0^\infty \int_{\Omega_{space}} \frac{2\nu^2}{c^3} \frac{\varepsilon_D h\nu}{e^{\frac{h\nu}{kT_D}}-1} d\Omega d\nu \quad (8)$$

where T_B is the background temperature, probably 0K, ε_D is the emissivity of the detector into free space which can be a function of ν and Ω, ε_{ED} is the coupling between emitter and detector in the cavity, and Ω_{space} represents the solid angle distribution of detector emission outside the cavity, (i.e. $4\pi - \Omega_{cav}$, where Ω_{cav} represents the solid angle distribution of the cavity modes). Note that we do not need to include the emitter fluctuations to the background in the equation because it is only the detector that is observing the fluctuations, so only interactions that couple directly to the detector are relevant. See Fig. 3 for a conceptual diagram of the cavity geometry. The first term on the left hand side represents the energy emitted from the emitter to detector, the second term on the left side represents the energy emitted from the background to the detector, the first term on the right represents the energy emitted from detector to emitter, and the second term on the right side represents the emission from detector to background. Of these terms, the emission from detector to emitter ($T_D << T_E$) and the emission from the background ($T_B \sim 0K$) to the detector can be neglected in an idealized analysis, in which case we can rewrite the above as:

$$\sum_{\mathrm{m}} \frac{\varepsilon_{ED} h\nu}{e^{\frac{h\nu}{kT_E}}-1} = \int_0^\infty \int_{\Omega_{space}} \frac{2\nu^2}{c^3} \frac{\varepsilon_D h\nu}{e^{\frac{h\nu}{kT_D}}-1} d\Omega d\nu \quad (9)$$

We have assumed that the volume surrounding the open-sided cavity is large enough to be considered free space. This is not a necessary condition, but it does allow us to maximize the peripheral mode number and therefore minimize the equilibrium detector temperature in a radiation-limited system.

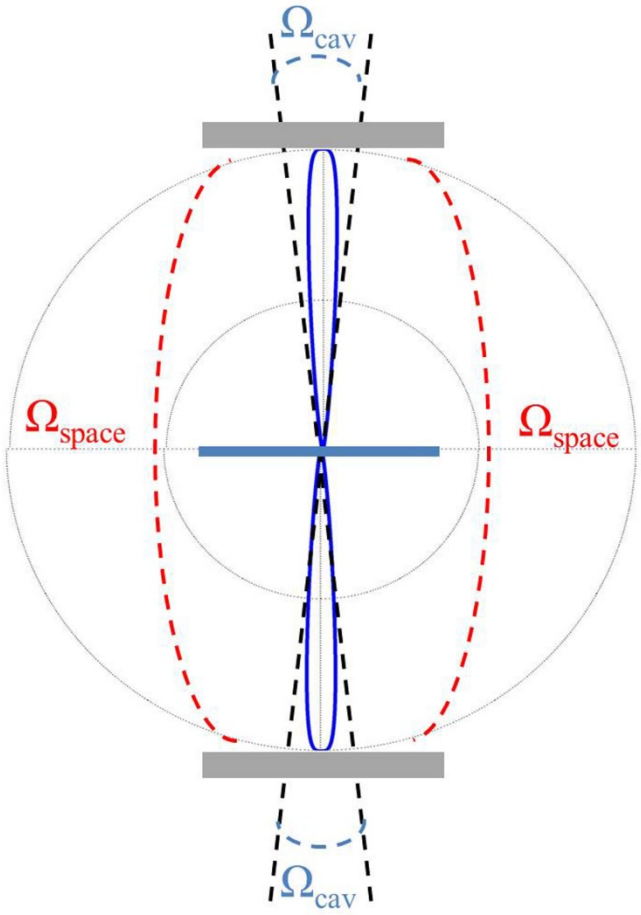

FIG. 3 (color online). Diagram of the solid angles used in noise and radiation heat transfer calculations of a single cavity containing a coupled emitter and detector.

From the above equation, if we select a temperature, T_E, for the emitter, say by introducing a joule heating current into the emitter plate, then we can calculate the steady-state detector temperature. Once we have determined this, we can estimate the energy fluctuations and radiation noise of the system. The detector will have two dominant sources of radiation noise: absorbed radiation from the emitter via the fundamental cavity mode, and emitted radiation from the detector itself due to its finite temperature, T_D. This latter noise is emitted to all available modes, not merely those aligned along the cavity axis, and since the number of peripheral modes can be very high, they will usually dominate the detector emission fluctuations. In order to measure only the radiation noise in the few (or one) modes along the cavity axis, the emitter radiation fluctuations must greatly exceed the detector emitted fluctuations, $\langle \Delta E^2 \rangle_{emitter} >> \langle \Delta E^2 \rangle_{detector}$. Calculating this condition involves integrating the energy fluctuations for the detector (right hand side) over all modes and space and then solving for T_D for a given T_E such that

this is much less than the energy fluctuations of the emitter (left hand side) in the relevant cavity mode(s):

$$\sum_{\mathrm{m}}(h\nu)^2\left[\frac{\varepsilon_{ED}}{e^{\frac{h\nu}{kT_{\mathrm{E}}}}-1}+\left(\frac{\varepsilon_{ED}}{e^{\frac{h\nu}{kT_{\mathrm{E}}}}-1}\right)^2\right]_{\mathrm{m}} \quad (10)$$
$$>>\int\int_{\Omega_{space}}\frac{2\nu^2}{c^3}(h\nu)^2\left[\frac{\varepsilon_D}{e^{\frac{h\nu}{kT_{\mathrm{D}}}}-1}+\left(\frac{\varepsilon_D}{e^{\frac{h\nu}{kT_{\mathrm{D}}}}-1}\right)^2\right]Vd\Omega d\nu$$

In the above expression, we have again neglected the background emission everywhere and detector emission in the main cavity modes because any practical solution to the above condition will require T_B to be small and $T_E >> T_D$; therefore, the detector fluctuations in the cavity and the background fluctuations elsewhere will be negligible. Note that the above expression is a conservative estimate for measurability because we have assumed that any emission outside the main cavity axis occurs into free space; emission into a more limited volume will involve a smaller mode density and thus a smaller contribution to energy fluctuations, improving our prospects of detecting BE-like noise.

In Fig. 4, we show solutions for Eqns (9) and (10) for a single mode half-wave cavity at various resonance wavelengths, using the condition that the "much greater than" symbol refers to exactly one order of magnitude. In this plot, we have changed the emitter temperature, T_E, in the single mode cavity by, for example, introducing a controlled current to induce joule heating. The detector temperature is forced to a finite value by radiation transfer from the emitter. For simplicity, the background has been assumed to be at T=0K. At this point, we know the temperature of both the emitter and detector for purely radiation-limited heat transfer. We can now calculate from the maximum detector temperature that will allow the radiation background noise measured by the detector to be dominated by received radiation from the emitter, as predicted by Eqn (10). Domination by the emitter is crucial since, at a given wavelength, higher temperature objects will have a stronger BE component to their photon statistics and the emitter-detector coupling only covers one or a small number of modes, making BE statistics observable. From this data, we can see that at almost all elevated temperatures, *the maximum acceptable detector temperature is lower than can be achieved in a radiation-limited system, which means that we must have some degree of detector cooling via heat conduction*. Note that this conclusion is relatively independent of cavity finesse.

In addition to the above analysis, the solutions of Eqns. (9) and (10) in Fig. 4 actually meet at ultra-low temperatures. Since the number of thermal photons in this regime becomes negligibly small, vacuum fluctuations would dominate. However, the variance due to virtual photons can only be considered if detector sampling period is within the order of lifetime of virtual photons [37]. Their lifetime is upper limited by the uncertainty principle [38]

$$\Delta \mathrm{E}\Delta t \approx \frac{h}{2\pi} \quad (11)$$

where h is Planck's constant, ΔE is the energy of virtual photons and Δt is the existing period of those photons. ΔE is around 0.248eV if $\lambda = 5\mu m$, so the effective photon "lifetime" Δt is around 0.25fs. We will discuss this point in relation to cavity lifetime later.

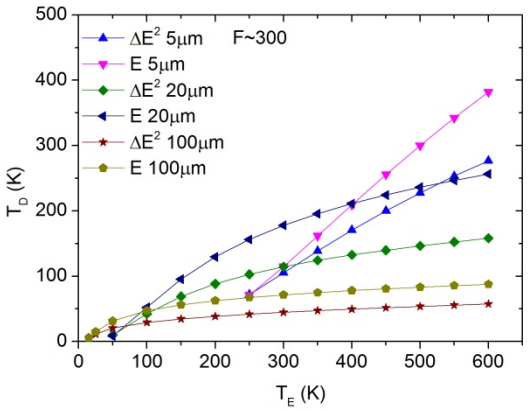

FIG. 4 (color online). Plots of (**E**) the detector temperature versus emitter temperature for a single isolated cavity and (**ΔE^2**) the maximum detector temperature such that overall detector energy fluctuations are dominated by received power from the emitter (an order of magnitude greater than other sources). When the emitter is heated, it gives off radiation, some of which is absorbed by the detector. This raises the temperature of the detector to an equilibrium temperature, T_D. The detector then has a radiation noise with contributions from fluctuations in the received emitter energy and the fluctuations of its own emitted energy. To observe BE noise, the former should dominate, and in these plots, that is not the case if radiation heat transfer is the only mechanism determining T_D. Some external cooling mechanism must be used to meet the condition of Eqn (10). The curves are solutions for Eqns. (9) and (10) for a single mode half-wave cavity at various resonance wavelengths with A_E=0.005 and A_D=0.005. The cavity can be considered as similar to that in Fig. 1(a).

Figures 6-9 quantify the radiation background fluctuations for a single cavity system as a function of emitter temperature, finesse, cavity resonant wavelength, and number of longitudinal modes. In each case, the actual energy fluctuations are compared to the case of a perfect Poisson system and an extreme BE system (where $\langle \Delta n^2 \rangle \sim \langle n \rangle^2$). The data above

establishes that, for a cavity with total isolation in one dimension, the primary criteria for observability for BE background noise in a single cavity are 1) a high emitter temperature, 2) an extremely long observation wavelength, and 3) a sufficiently low detector temperature relative to the emitter.

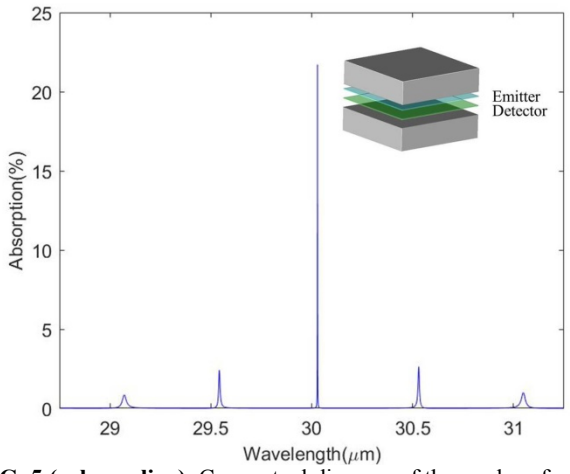

FIG. 5 (color online). Conceptual diagram of the modes of a single cavity containing an emitter and detector of the type shown in Fig. 1 (a). The simulations of Figs. 6-9 are based on variations around this basic cavity. TABLE I describes the layer structure in detail. The layers include 5.5 pairs of $3\mu m$ n=2.5 and $6\mu m$ n=1.25, $135\mu m$ n=1, 60nm n=2-2i, $750\mu m$ n=1 (A), another 60nm n=2-2i, $15.75\mu m$ n=1, and 9.5 pairs of $3\mu m$ n=2.5 and 6μm n=1.25. Here, a non-dispersive (constant) refractive index has been assumed for both the emitter and detector. A frequency-dependent refractive index may change the heights and/or spacings of the peaks slightly.

TABLE I. Layer structure for the 5-mode single cavity of Fig. 5 at $30\mu m$.

	Thickness (μm)	Index	
5.5 pairs	3/6	2.5/1.25	
1	135	1	
1	0.06	2-2i	Detector
1	750	1	A
1	0.06	2-2i	Emitter
1	15.75	1	
9.5 pairs	3/6	2.5/1.25	

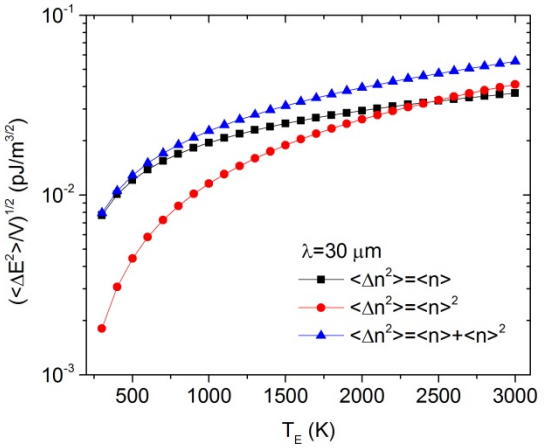

FIG. 6 (color online). Radiation background fluctuations as a function of emitter temperature for an isolated single cavity containing an emitter and detector. The plots for $\langle n \rangle$ and $\langle n \rangle^2$ are merely to show the relative importance of each term in the overall noise of the system, which is based on $\langle n \rangle + \langle n \rangle^2$. TABLE I describes the layer structure. Also, adjust length of A in TABLE I to obtain $n\lambda/2$ and volume.

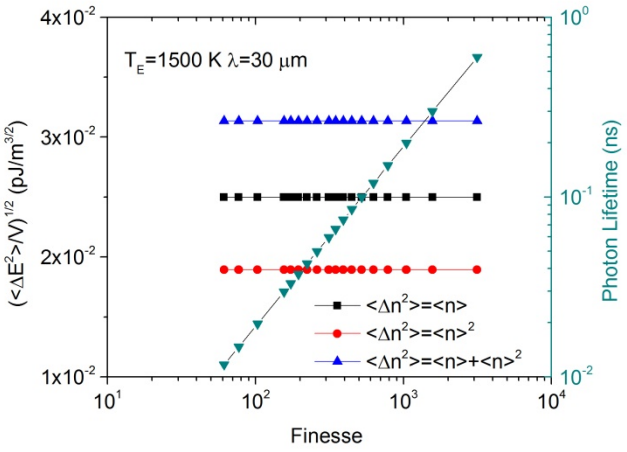

FIG. 7 (color online). Radiation background fluctuations as a function of finesse for an isolated single-mode cavity containing an emitter and detector. Since there is only one mode regardless of spectral width and the detector is at a low enough temperature that it does not emit significant radiation to the peripheral background, the fluctuations are constant. The plots for $\langle n \rangle$ and $\langle n \rangle^2$ are merely to show the relative importance of each term in the overall noise of the system, which is based on $\langle n \rangle + \langle n \rangle^2$. TABLE I describes the layer structure. Also, adjust length of A in TABLE I to obtain $n\lambda/2$ and volume.

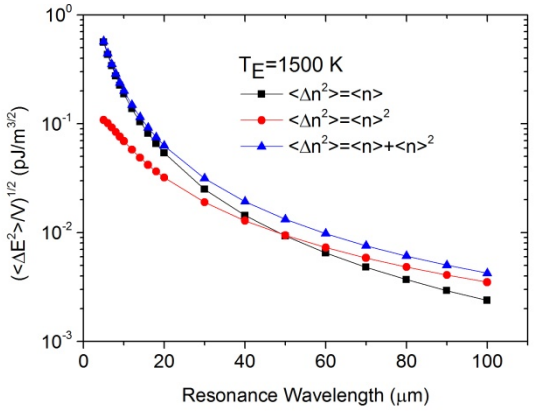

FIG. 8 (color online). Radiation background fluctuations for a single cavity system as a function of cavity resonant wavelength. Note that the actual fluctuations ($\langle n \rangle + \langle n \rangle^2$) are indistinguishable from Poisson statistics for wavelengths less than about $10\mu m$ and only become clearly differentiated above $20\mu m$. TABLE I describes the layer structure. Also, adjust length of A in TABLE I to obtain $n\lambda/2$ and volume.

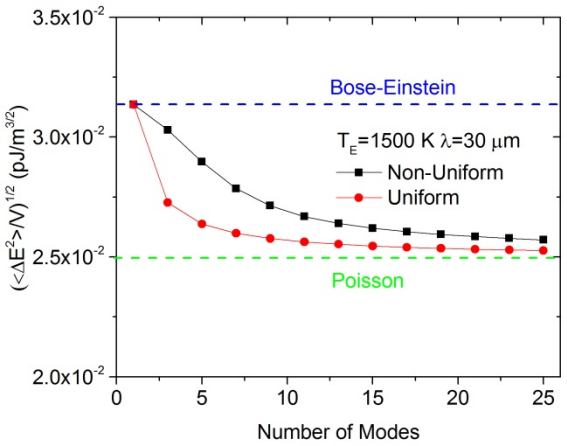

FIG. 9 (color online). Radiation background fluctuations for a single cavity system as a function of longitudinal modes. In this plot, we have taken the same cavity system from Figs. 6-8, except that the length has been increased to introduce additional modes into the detector absorption pass band. The "Non-Uniform" curve represents the data of interest, while "Uniform" curve refers to a hypothetical system where all modes couple equally to the emitter and is included for comparison. TABLE I describes the layer structure. Also, adjust length of A in TABLE I to obtain $n\lambda/2$ and volume.

Interestingly, cavity finesse is essentially irrelevant in the case of the isolated resonator because the average number of photons is determined by the number of modes, not the spectral width of any mode resonance. Spectral width is only involved when there is another space with modes with which the cavity could couple. However, cavity finesse plays a very important role in determining the photon lifetime of a system. This is important because any fluctuation in the mode energy is by its nature very transient. A deviation of the number of photons from average will exist on average for only a photon lifetime. This means that any detector hoping to see these fluctuations must operate with a response time on the order of the photon lifetime or faster. Otherwise, the noise will be observed as an average over many photon lifetimes, which will revert the statistics to Poisson-like behavior. Additional discussion of detectors will be delayed to later.

On a related note, vacuum fluctuations have a lifetime with an upper bound given by the uncertainty principle, which makes their "lifetime" enormously shorter than the lifetime of real photons. This would make the vacuum variance in a thermal cavity essentially impossible to see. However, if one dispenses with low energy microsystems (i.e. thermal cavities as in this paper), and instead turns to an ultra-fast, high energy system: a femtosecond laser, then one can actually see the effects of the vacuum field variance. An interesting recent work, Reference [37], shows that the effects of the vacuum field variance can be observed through the extreme nonlinearities produced by a high brightness femtosecond laser. Here, enormous electric fields are produced in a tiny volume for a time period much less than a single cycle of the emission wavelength.

We note that the wavelength needed to observe BE-like noise is longer than would be expected from a simple calculation using Eqn (3). Instead, Eqn (4) must be used because of the imperfect coupling between the emitter and detector, ε_{ED}. The required long wavelengths make the isolated single cavity case most compatible with a THz resonator, although differences between Poisson and BE will be visible in the long-wavelength infrared as well.

One additional question that deserves discussion is whether it would be possible to see BE-like noise using outcoupled light from a high finesse resonator via a coupled waveguide or scattering defect without the need to include a detector inside the resonator. This is definitely possible, but will run into the issue raised in conclusion 2 from our thermal emission discussion earlier in the paper. As one samples a photon population, one is reducing the number of observed photons to well below the actual number in a mode. Since the BE component of noise relies on $\langle n \rangle^2$, our ability to distinguish BE from Poisson becomes much more difficult. On the other hand, a large sample cannot be outcoupled (at least in steady-state) from the primary resonator mode because this loss will then limit the isolation of the resonator, causing it to interact more strongly with the modes of the environment. Truly a conundrum!

Another issue with waveguide outcoupling is that an extremely long length waveguide introduces many modes onto the propagation axis, while a shorter waveguide develops tunneling modes as the length decreases, eventually approaching near-free-space densities as the length becomes very short.

B. Observing Bose Einstein radiation background noise in coupled spaces

It is also possible to observe BE-like noise in two coupled cavities as we will now argue. Consider, the configuration of Fig. 1(b). Here a single mode cavity containing a heated emitter is coupled to an external observing space containing a cryogenically cooled detector. This detector will be assumed to cold shielded and filtered so that it is only responsive to the spectral emission of the fundamental mode of the emitter cavity. The detector cavity will contain many modes, the number of which will be determined by the size of the cavity, which is a variable that we will control. For simplicity, we will assume a cavity that has lateral dimensions of $\lambda/2$ by $\lambda/2$, but with a length of $n\lambda/2$, where n is an integer that we can control to alter the volume of the cavity. In this system, the walls of the detector cavity have perfect reflectivity, $R_d=1$, but the detector itself has an absorption and is positioned as shown in the inset of Fig. 10 and described in TABLE II. The emitter cavity has a perfectly reflecting back mirror, $R_b = 1$, but a front mirror, that is, the mirror that couples the emitter and detector cavities, that has a reflectivity, $R_f < 1$. In this way, the two cavities are coupled to one another but completely isolated from the outside world. The single mode version of this coupled cavity system has a photon lifetime of 0.14ns.

The volume (determined by length in our specific example) of the detector plays a dominant role in how many modes interact with the emitted photons and thus the amount of BE behavior that will be seen in the noise. However, R_f and the absorptions of the detector and emitter also have a large effect since they help determine the width of the resonances within the emission envelope, as shown in Fig. 10. In this figure, a system is shown where approximately five detector cavity modes couple at some level with the emitter resonance. In Fig. 10, the resonances are shown as extremely narrow, but these would widen if the single-pass absorption of the detector, A_d, could be hypothetically increased without affecting the other parameters of the cavity. This concept is shown in Fig. 11. As A_d increases, coherent interactions decrease, and the resonances widen. In the case of extremely high detector absorption, where A_d approaches 1, the width of the resonances that originate with the detector widen towards infinity and the coupling peak-to-valley difference (frequency dependence of coupling) decreases as the valley minima move towards perfect absorption. This effectively creates a uniform mode structure in the cavity system. When the detector resonances are very narrow compared to the emitter resonance, each mode couples differently, and we must turn to the effective mode calculation discussed previously in order to calculate the noise fluctuations, as shown in Fig. 12. Figure 13 shows the noise fluctuations as a function of cavity volume for the ideal cases of Poisson statistics, BE statistics, and uniform modes, and the actual case of coupled modes. Figure 13 shows the plot for T_E = 1500K at $\lambda = 50\mu m$. As with the single cavity case, we can see that distinguishing BE from Poisson statistics is still difficult at short infrared wavelengths. At $5\mu m$, a difference of less than 3% is seen in a single mode system. At longer infrared wavelengths, however, as shown in Fig. 13, and into the THz range, the distinction between BE and Poisson is very clear if a single or few mode system can be created.

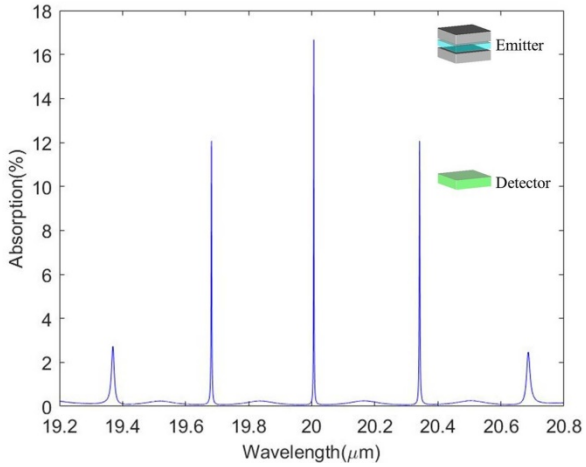

FIG. 10 (color online). Conceptual diagram of the modes of two coupled cavities as shown in the inset. The short cavity contains the emitter at elevated temperature and the second cavity the detector. The photon lifetime of this coupled cavity system is 0.14ns. TABLE II describes the layer structure in detail. The layers include 4.5 pairs of $2\mu m$ n=2.5 and $4\mu m$ n=1.25, $600\mu m$ n=1 (A), 40nm n=2-2i, another $600\mu m$ n=1 (B), 2.5 pairs of $2\mu m$ n=2.5 and $4\mu m$ n=1.25, $8\mu m$ n=1.25, 1.5 pairs of $2\mu m$ n=2.5 and $4\mu m$ n=1.25, $5\mu m$ n=1, 20 nm n=2-2i, another $5\mu m$ n=1, and 9.5 pairs of $2\mu m$ n=2.5 and $4\mu m$ n=1.25. Here, a constant refractive index with frequency for both the emitter and detector is assumed. A dispersive refractive index would alter the heights and/or spacing of the peaks slightly.

TABLE II. Layer structure for the 5-mode coupled cavity at $20\mu m$.

	Thickness (μm)	Index	
4.5 pairs	2/4	2.5/1.25	
1	600	1	A

1	0.4	2-2i	Detector
1	600	1	B
2.5 pairs	2/4	2.5/1.25	
1	8	1.25	
1.5 pairs	2/4	2.5/1.25	
1	5	1	
1	0.02	2-2i	Emitter
1	5	1	
9.5 pairs	2/4	2.5/1.25	

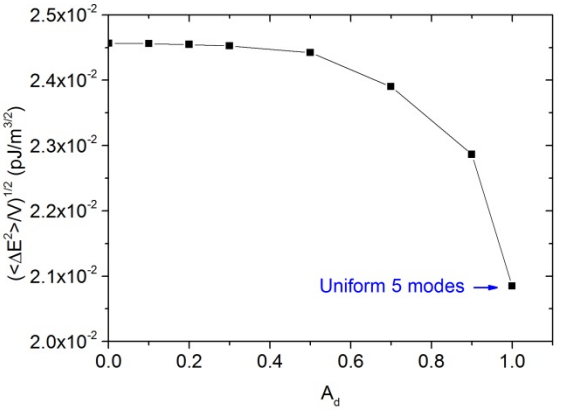

FIG. 11 (color online). Plot of energy fluctuations versus detector absorption for a basic coupled-cavity system in the case where 5 modes have been coupled to the detector. The emitter cavity parameters are: R_1=0.999, R_2=1, A=0.001, $L = 10\mu m$, and T=1500K. As the detector absorption increases, the coupled resonances become broader, effectively becoming uniform as A_d approaches one.

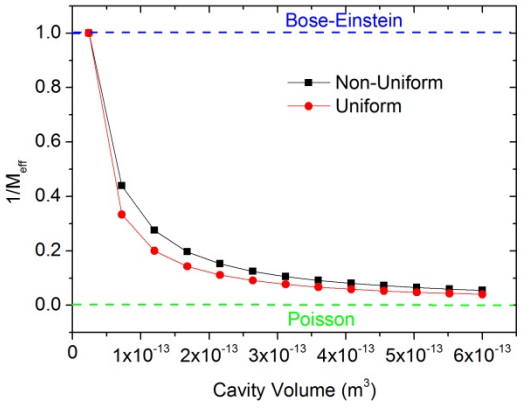

FIG. 12 (color online). Plot of inverse effective mode number versus cavity volume for the basic coupled cavity of Fig.10. For comparison, plots of a perfect BE system (M = M_{eff} = 1), a perfect Poisson system (M = M_{eff} = ∞), and a uniform mode system (M_{eff} = M) have been made. TABLE II describes the layer structure. Also, adjust length of A and B in TABLE II to obtain $n\lambda/2$ and volume.

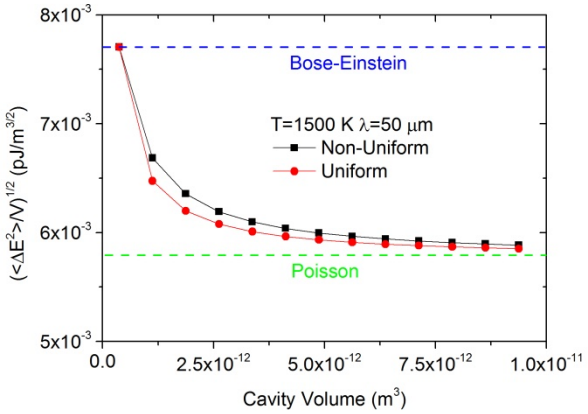

FIG. 13 (color online). Energy fluctuations versus cavity volume for a coupled cavity system with the basic structure of Fig. 10 for a center wavelength of $50\mu m$. For comparison, plots of a perfect BE system (M = M_{eff} = 1), a perfect Poisson system (M = M_{eff} = ∞), and a uniform mode system (M_{eff} = M) have been made. TABLE II describes the layer structure. Also, adjust length of A and B in TABLE II to obtain $n\lambda/2$ and volume.

Before concluding, it is useful to speculate on the chances of observing BE-like statistics in thermal emission. This analysis has shown that such observation is possible in theory. The magnitudes of the differences between Poisson-like and BE-like noise become quite significant under the right conditions. However, there are significant practical difficulties. The first involves the spectral regime. BE-like noise will only dominate over Poisson-like noise for emitters at elevated temperatures and systems operating at long wavelengths. For example, this paper used $\lambda \sim 30\mu m$ and T_E = 1500K, and ranges with temperatures and wavelengths scaled appropriately or higher/longer are viable. Interestingly, the finesse requirements of cavities or resonators are not a major factor in the success or failure of BE-like noise detection. Unfortunately, though, the materials and device technologies for the above wavelength ranges are not nearly as advanced as in the visible and near-IR. There are few materials that could be fabricated into modally isolated far-IR cavities. Possibilities include diamond and ionic solids such as KBr, but significant technological development would be necessary to create low-loss high reflectivity coatings and resonators. Metallic or metamaterial resonators in the THz perhaps provide a better path forward as they can be isolated from external world by the metal of the resonator itself. Small metallic losses within the resonator are acceptable for mode coupling as the finesse needs to be high enough to ensure that the coupling of the system is dominated by the emitter and detector, but not so high that finesses typical of near-IR microresonators are necessary. However, there are significant photon lifetime issues introduced by the

finesse. As mentioned previously, any detector must be able to sample the photon number of the system with a response lifetime comparable to or faster than the photon lifetime. Although the photon lifetime varies wildly depending on the cavity design, a value on the order of 100ps is a reasonable working number. At infrared frequencies, the number of photons in a mode dominated by BE-like statistics will be slightly greater than one. (There may be several or more photons on average for a mode in the THz.) This means that detectors must be able to distinguish individual photons in the infrared at speeds compatible with the photon lifetime. This would be a difficult task even for cryogenically cooled telecommunications-grade technology; in the far-infrared and THz, such detector technology is not currently available.

IV. CONCLUSION

In this paper, we have developed relationships to describe radiation background noise for micro- and nano-resonators that applies to any arbitrary cavity mode structure, including coupled systems. It is shown that the noise analysis of few-mode systems differs substantially from ideal treatments in prior art (free space coupling, uniform mode structure, and Poisson-only statistics). With this theory, it has been shown that the photon statistics of a system of modes can be extracted as a sum over the statistics of the individual modes of the systems, weighted by coupling coefficients that turn out to the be the emissivities of each individual mode, as one would expect from Kirchoff's Law.

The theory has been used to quantitatively analyze the possibility of seeing Bose-Einstein noise behavior in thermal emission, a process that has long been predicted for single mode systems but never experimentally observed. Both single isolated cavities containing an emitter and detector and coupled cavities with emitter and detector separated in different cavities have been treated. It is concluded that for emission into free space, the possibility of observing BE-like noise from micro- and nano-resonators is very low because a level of spectral purity is required that is far beyond anything that has been experimentally demonstrated to date. It is shown that BE-like noise can indeed be seen at high temperatures and long wavelengths for isolated and coupled cavities, but ironically, resonator finesse seems to play little role in these cases, as it is primarily the mode isolation that enables BE observability. The optimal wavelengths for observing BE-like noise in isolated and coupled cavities begin in the long-wavelength infrared towards the transition region to THz; BE-like noise should be visible for single mode resonators and those with mode numbers less than approximately five.

ACKNOWLEDGMENT

The authors gratefully thank the Army Research Office for funding under Grant No. W911NF-15-1-0243.

[1] S. J. C. Yates, J. J. A. Baselmans, A. Endo, R. M. J. Janssen, L. Ferrari, P. Diener, and A. M. Baryshev, Appl. Phys. Lett. **99**, 073505 (2011).
[2] P. J. de Visser, J. J. A. Baselmans, J. Bueno, N. Llombart, and T. M. Klapwijk, Nat. Commun. **5**, 3130 (2014).
[3] J. Hubmayr, J. Beall, D. Becker, H.-M. Cho, M. Devlin, B. Dober, C. Groppi, G. C. Hilton, K. D. Irwin, D. Li, P. Mauskopf, D. P. Pappas, J. Van Lanen, M. R. Vissers, Y. Wang, L. F. Wei, and J. Gao1, Appl. Phys. Lett. **106**, 073505 (2015).
[4] S. R. Andrews and B. A. Miller, J. Appl. Phys. **70**, 993 (1991).
[5] A. Reiser and L. Schachter, Phys. Rev. A **87**, 033801 (2013).
[6] S. M. Rytov, Theory of Electric Fluctuations and Thermal Radiation (Air Force Cambridge Research Center, Bedford, 1959).
[7] R. W. Boyd, Infrared Phys. **22**, 157−162 (1982).
[8] S. Gulkis, TDA Prog. Rep. **42-71**, 53−59 (1982).
[9] R. C. Jones, J. Opt. Soc. Am. **37**, 879–888 (1947).
[10] P. B. Fellgett, J. Opt. Soc. Am. **39**, 970–976 (1949).
[11] W. B. Lewis, Proc. Phys. Soc. **59**, 34–40 (1947).
[12] P. Fellgett, C. Jones, and R. Q. Twiss, Nature **4691**, 967−969 (1959).
[13] M. Planck, Annalen der Physik **306**, 719–737 (1901).
[14] P. L. Richards, J. Appl. Phys. **76**, 1 (1994).
[15] P. W. Kruse, L. D. McGlauchlin, and R. B. McQuistan, Elements of Infrared Technology (Wiley, 1962).
[16] E. L. Dereniak and G. D. Boreman, Infrared Detectors and Systems (Wiley-Interscience, 1996).
[17] J. J. Talghader, A. S. Gawarikar, and R. P. Shea, Light Sci. Appl. **1**, e24 (2012).
[18] C. Wuttke and A. Rauschenbeutel, Phys. Rev. Lett. **111**, 024301 (2013).
[19] D. J. Benford, T. R. Hunter, and T. G. Phillips, Int. J. Infrared Millimeter Waves **19**, 931–938 (1998).
[20] K. Olson and J. Talghader, Phys. Rev. A **94**, 013822 (2016).
[21] P. Del'Haye, A. Schliesser, O. Arcizet, T. Wilken, R. Holzwarth and T. J. Kippenberg, Nature **450**, 1214–1214 (2007).

[22] T.-J. Wang, J.-Y. He, C.-A. Lee, and H. Niu, Opt. Express **27**, 28119−28124 (2012).
[23] M. Furchi, A. Urich, A. Pospischil, G. Lilley, K. Unterrainer, H. Detz, P. Klang, A. M. Andrews, W. Schrenk, G. Strasser, and T. Mueller, Nano Lett. **12**, 2773−2777 (2012).
[24] Y. Wang, B. J. Potter, and J. J. Talghader, Opt. Lett. **31**, 1945−1947 (2006).
[25] D. Kirikae, Y. Suzuki1 and N. Kasagi, J. Micromech. Microeng. **20**, 104006 (2010).
[26] Z. Su, N. Li, E. S. Magden, M. Byrd, Purnawirman, T. N. Adam, G. Leake, D. Coolbaugh, J. D. B. Bradley, and M. R. Watts, Opt. Lett. **41**, 5708−5711 (2016).
[27] Z. Qian, S. Kang, V. Rajaram, and M. Rinaldi, 2016 IEEE Sensors, 625−627.
[28] T. D. Dao, S. Ishii, T. Yokoyama, T. Sawada, R. P. Sugavaneshwar, K. Chen, Y. Wada, T. Nabatame, and T. Nagao, ACS Photonics **3**, 1271−1278 (2016).
[29] Eric W. Weisstein, CRC Encyclopedia of Mathematics Volumes II and III (3rd Ed., CRC Press, 2009).
[30] L. Mandel and E. Wolf, Optical Coherence and Quantum Optics (Cambridge University Press, 1995).
[31] M. Fox, Quantum Optics: An Introduction (Oxford University Press, 2006).
[32] Peter W. Milonni, The Quantum Vacuum An Introduction to Electrodynamics (Academic Press 1994).
[33] C. Lecaplain1, C. Javerzac-Galy, M.L. Gorodetsky, and T.J. Kippenberg, Nat. Commun. **7**, 13383 (2016).
[34] A. Rasoloniaina, V. Huet, T. K. N. Nguyên, E. Le Cren, M. Mortier, L. Michely, Y. Dumeige & P. Féron, Sci. Rep. **4**, 4023 (2014).
[35] P. Ma, D.-Y. Choi, Y. Yu, Z. Yang, K. Vu, T. Nguyen, A. Mitche, B. Luther-Davies, and S. Madden, Opt. Express **23**, 19969−19979 (2015).
[36] K. Olson, High Power Continuous Wave Laser Heating and Damage with Contamination, and Non-Uniform Spectrally Dependent Thermal Photon Statistics (Doctoral Dissertation, University of Minnesota, 2015).
[37] C. Riek, D. V. Seletskiy, A. S. Moskalenko, J. F. Schmidt, P. Krauspe, S. Eckart, S. Eggert, G. Burkard, A. Leitenstorfer, Science **350**, 420−423 (2015).
[38] Carlos I. Calle, Superstrings and Other Things: A Guide to Physics (2nd Ed., CRC Press, 2010).